PVT Measurement Methodology for Semicrystalline Polymers to Simulate Injection-Molding Process

J.-F. LUYÉ,[1] G. RÉGNIER,[1] PH. LE BOT,[2] D. DELAUNAY,[2] R. FULCHIRON,[3]

[1] Laboratoire de Transformation et Vieillissement des Polymères, ENSAM, Paris, France

[2] Laboratoire de Thermocinétique, ISITEM, Nantes, France

[3] Laboratoire des Matériaux Polymères et des Biomatériaux—UMR-CNRS 5627, UCBL-ISTIL, 43 Boulevard du 11 novembre 1918, 69622 Villeurbanne Cedex, France

Received 3 August 1999; revised 31 March 2000; accepted 4 April 2000

ABSTRACT: This article discusses the specific volume-measurement methods for semicrystalline polymers needed in order to obtain reliable data. Particularly, the effect of the cooling rate is analyzed, taking into account the thermal gradient in a cylindrical sample. Experimental results for a polypropylene form the basis for the study. In a first step our thermal model was validated by comparing the calculated results with the experimental ones for a temperature range higher than the crystallization zone with different cooling rates and by analyzing the stabilization time of the measured specific volume after cessation of the cooling. Secondly, specific-volume evolutions from 220°C to 50°C for different cooling rates and different pressures were analyzed, revealing that when the data are corrected to eliminate the thermal gradient effect, the transition zone is much narrower than the experimental one. Moreover, the effect of the pressure and the cooling rate on the relative crystallinity function—that is, on the crystallization kinetics—can be more accurately evaluated. © 2000 John Wiley & Sons, Inc. J Appl Polym Sci 79: 302–311, 2001

Key words: pressure–volume–temperature measurement; thermal study; crystallization; polypropylene

INTRODUCTION

In order to simulate the injection-molding process of polymeric materials, the knowledge and the modeling of their pressure–volume–temperature (PVT) behavior is essential. Indeed, prediction of the polymer quantity that enters the cavity is linked to the specific volume of the polymer for the corresponding pressure and temperature. Consequently, the pressure evolution during the cooling and even the volume shrinkage will be affected. The particularity of PVT behavior for polymers is that the transition region between liquid and solid states is strongly dependent on the measurement conditions. For example, in the case of amorphous polymers, the transition zone, that is, the glass transition, is influenced by the pressure[1] (0.2–0.5°C/MPa) and even by the cooling or heating rate.[2]

In the case of semicrystalline polymers, the problem is even more difficult. Indeed, the crystallization temperature is always different than the melting temperature because the occurrence of crystallization requires a great supercooling[3] (several tens of degrees). Moreover, the crystallization temperature is very dependent on the cool-

Correspondence to: R. Fulchiron.

Journal of Applied Polymer Science, Vol. 79, 302–311 (2001)

ing rate and the pressure. Furthermore, the final crystallinity can substantially depend on the crystallization conditions, leading to various solid-state-specific volumes. Hence, the measured specific volume at one temperature and one pressure is the result of the entire thermal and pressure histories. Consequently, the PVT data appear dependent on the measuring method. In this article, after reviewing the different PVT measurement procedures and techniques, we show how to take experimental results and isolate the material PVT behavior by taking into account the thermal gradient in the sample.

Measuring Procedures

The different procedures to obtain a PVT diagram can be listed as:

(1) *Isothermal compressing taken in order of increasing temperature:* the specific volume is recorded along isotherms (in order of increasing temperature) and at different pressures. Between each temperature there is a stabilization time of a few minutes before the next isotherm. This procedure is often considered the "standard" one.
(2) *Isothermal compressing taken in order of decreasing temperature:* the procedure is the same as case (1), but the isotherms are in order of decreasing temperature.
(3) *Isobaric heating:* The specific volume is recorded along isobars with a fixed heating rate.
(4) *Isobaric cooling:* The specific volume is recorded along isobars with a fixed cooling rate.

First, since in injection molding the polymer enters the cavity in the melt state and is cooled in the mold, it seems obvious that the transition that must be considered is crystallization. So procedures (1) and (2) appear inconvenient because they show the melting transition even if procedure (1) is often used.

Second, procedures (1) and (2) exhibit a single transition temperature (respectively, melting and crystallization temperatures) independent of the pressure. Nevertheless, this phenomenon is in total contradiction with thermodynamics because both melting and crystallization temperatures are increased by the pressure.[2] Actually, the single observed transition temperature is explained by the following arguments: When the isotherms are followed in the order of increasing temperature, the polymer melts for a given temperature at the lower pressure. Then, when the pressure is increased, it does not have enough time to recrystallize because the crystallization is very slow in this range of temperature. Therefore, the apparent melting temperature on the PVT diagram corresponds to the lowest pressure used in the procedure. When the isotherms are followed in the order of decreasing temperature, due to the thermodynamics, crystallization occurs at a given temperature for the highest pressure (at the end of the isotherm if the pressures are scanned in increasing order). Then, when measuring the next point—that is, the lowest pressure and the next lowest temperature—the polymer is already crystallized, but generally the temperature is lower than the melting point corresponding to this pressure so it cannot melt. Therefore, the apparent single crystallization temperature coincides with the crystallization temperature for the highest pressure used in the procedure. Moreover, since crystallization can be a very slow phenomenon, it can either occur or not occur depending on the chosen stabilization time between two temperatures.

For all the previous reasons, the best procedure seems to be isobaric measurements in cooling mode, procedure (4), because in that case the observed transition is the crystallization, and it depends only on the pressure and the cooling rate. The effect of the cooling rate can be investigated. Nevertheless, as it will be shown further, the analysis of the data still faces a difficulty because of the thermal gradient that occurs in the sample, complicating the effect of the cooling rate on the crystallization kinetics. Therefore, thermal analysis of the data is the main focus of this article.

PVT Devices

The two main PVT measurement techniques are immersion of the sample in a fluid and measuring the length of the sample between two pistons. In the first technique, made commercial by GNOMIX (Boulder, CO),[1,3] a sample, typically 1–2 g, is placed in thin nickel foil and then immersed in mercury. Pressure is then applied to the mercury. This technique ensures a real hydrostatic pressure on the sample.

With the second technique, used in the current study, the sample is put in a cylindrical cell, and the specific volume is deduced from the measured length of the sample. The experimental results of

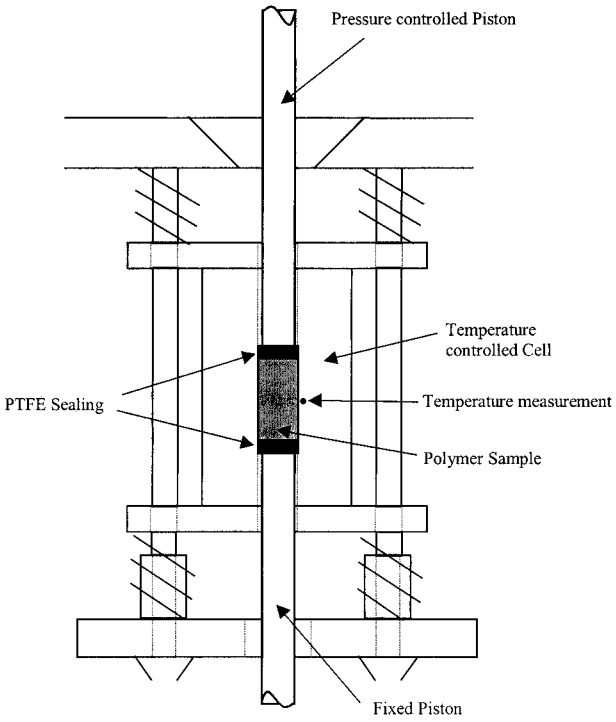

Figure 1 Schema of the PVT cell.

this work were obtained with an apparatus (PVT100) manufactured by the German supplier SWO Polymertechnik GmbH (Krefeld, Germany). A schematic of this device is shown in Figure 1. The typical weight of the sample is 0.5–1 g. The diameter of the cell is 7.4 mm. The lower piston is fixed, and the upper one can move, ensuring the pressure. Between each piston and the sample is a PTFE sealing to avoid leakage. The measurement of the upper piston displacement provides the length of the sample after subtraction of the sealing volume. The temperature control of the cell is ensured by an electric heater band, and the cooling is by air. The temperature is measured using a thermocouple placed very near the sample. Moreover, the cell is mounted on springs allowing relative movements between the cell and the pistons. In this way, the pressure is always applied on both sides of the sample, even if it sticks on the cell (all the normal force is transmitted to the lower piston).

This technique's main disadvantage is not ensuring a hydrostatic pressure on a sample in the solid state. Considering a purely elastic material in the solid state, Lei et al.[4] compared the decreasing of a specific volume with a pressure increase from the atmospheric pressure up to a pressure, P, measured both with the piston technique (ΔV_{pist}) and in a hydrostatic condition (ΔV_{hydro}). They obtained the expression of the ratio λ_v:

$$\lambda_v = \frac{\Delta V_{pist}}{\Delta V_{hydro}} = \frac{1+\nu}{3(1-\nu)} \quad (1)$$

where υ is the Poisson coefficient.

From this equation the relative difference (e) of specific volumes given by the two techniques can be expressed as follows:

$$e = \frac{V_{pist} - V_{hydro}}{V_{hydro}} = \frac{V_0 - \Delta V_{pist} - V_0 + \Delta V_{hydro}}{V_0 - \Delta V_{hydro}} = \frac{1-\lambda_v}{V_0/\Delta V_{hydro} - 1} \quad (2)$$

where V_0 is the specific volume at ambient temperature and pressure.

In this equation, the ratio $V_0/\Delta V_{hydro}$ is obtained by:

$$V_0/\Delta V_{hydro} = V_0 \Big/ \left(\frac{V_0 P}{K}\right) = \frac{E}{3P(1-2\nu)} \quad (3)$$

where P is the pressure, K is the bulk modulus, and E is Young's modulus.

Let us consider typical temperature values above the glass-transition temperature of a polymer. For polypropylene, the polymer studied in this work, we get (υ = 0.42, E = 1.4 GPa), λ_v = 0.816. For a pressure of 120 MPa, which is the maximum pressure used in this study, the relative difference, e, is then 0.8%. However, when the pressure is higher than 20 MPa, which is the lowest pressure allowed by the device, the applied stress is largely greater than the elastic limit of such a material. Therefore, the purely elastic model used for eq. (1) is not valid anymore. Indeed, in that case, consideration should be given to viscoelastic behavior that obviously leads to a much lower error. From this analysis it can be concluded that for our purpose, the error from nonhydrostatic pressure is very small. The problem would obviously be more important for a glassy material of lower Poisson coefficient and higher yield stress.

As was mentioned before, the main purpose of this article is to show a method for analyzing the PVT diagrams obtained with different cooling rates in order to distinguish the effect of the thermal gradient in the sample from the effect of the

cooling rate on the crystallization kinetics. Indeed, it can be inferred from the size of the sample in the PVT apparatus that the temperature in the sample core is different from the temperature measured at the periphery by the thermocouple that's used as a reference. From this point of view, a measuring system with a cylindrical cell and two pistons is convenient because the geometry of the sample is well known, while with the immersion method, the sample's shape is free, leading to more difficult modeling. In addition, using the piston device produces a higher imposed cooling rate at the sample periphery than does the immersion system: typically up to 30°C./min^{-1} in the former case and a few degrees min^{-1} in the latter case.

Theoretical Considerations

The specific volume of a polymer can be written as follows:

$$V = \alpha V_s + (1 - \alpha)V_a \tag{4}$$

where V_a is the specific volume of the amorphous polymer, V_s is the specific volume of the solid polymer, and α is the relative mass crystallinity defined by

$$\alpha = \frac{X_c}{X_\infty} \tag{5}$$

where X_c is the crystallinity and X_∞ is the crystallinity at the end of the solidification.

In eq. (4), the specific volume of the solid polymer (V_s) can be expressed by

$$V_s = X_\infty V_c + (1 - X_\infty)V_a \tag{6}$$

where V_c is the specific volume of the pure crystalline phase.

The variation of the crystalline-phase specific volume with temperature and pressure is often considered as negligible compared to the amorphous phase because of a lack of data, but this assumption may be doubtful. Nevertheless, in the framework of this article, such an assumption is not necessary. It can be mentioned that X_∞ can depend on crystallization conditions, especially for polymers with slow crystallization kinetics. In other words, crystallization conditions influence both crystallization kinetics and solid-state specific volume (V_s). However, in this study, X_∞ does not affect our analysis because it does not need to be known.

When the specific volume is expressed for a temperature higher than the glass-transition temperature, the specific volumes V_a and V_s can be described by linear relations:

$$V_a = A_1(P) + A_2(P)T$$
$$V_s = A_3(P) + A_4(P)T \tag{7}$$

It is not the purpose of this article to describe the variations of the specific volume with the pressure. So the coefficients $A_1(P)$ to $A_4(P)$ will be used as discrete values for each pressure. Nevertheless, the use of a continuous equation to express the pressure and temperature dependence of the specific volume could be considered, if needed, without any difficulty. For example, different equations of state, such as the Tait equation[5,6] or Spencer and Gilmor–modified equation,[7] could be used.

The key point in eq. (4) is the relative crystallinity function (α) because of the great dependence of crystallization kinetics on temperature, pressure, and time (i.e., cooling rate). Using this point of view, this study deals with weighting of the thermal gradient as a result of experimental technique and with crystallization kinetics from intrinsic polymer properties. The work does not aim to analyze the crystallization kinetics phenomenon itself. So relative crystallinity variations with the cooling rate and the pressure will be taken into account only by a shift on the temperature scale.

EXPERIMENTAL

The polypropylene studied in this work is of a commercial injection grade supplied by Solvay (PP ELTEX HV252 MFI:11).

The primary relative crystallinity function [$\alpha(T)$] at atmospheric pressure was obtained from a DSC experiment using a DSC7 device from Perkin-Elmer. The sample was melted at 240°C and then cooled under a constant cooling rate of 5°C/min. The relative crystallinity was then obtained by integrating the crystallization peak between the temperature of the crystallization onset, T_i, and the temperature of the crystallization end, T_f . This relative crystallinity is plotted in Figure 2:

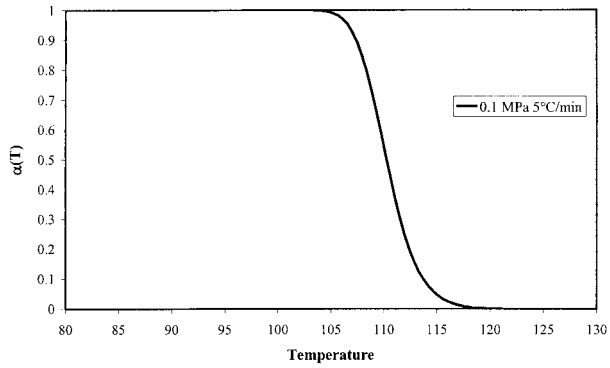

Figure 2 Primary relative crystallinity function obtained from DSC measurement at atmospheric pressure with a cooling rate of 5°C/min.

$$\alpha(T) = \frac{\displaystyle\int_{T_i}^{T} \left(\frac{dH}{dT}\right) dT}{\displaystyle\int_{T_i}^{T_f} \left(\frac{dH}{dT}\right) dT} \tag{8}$$

First, to test the validity of the thermal model, specific volume measurements were carried out in temperature domains where crystallization did not appear (220°C–180°C). Evolution of the specific volume was recorded using three cooling rates (5, 10, and 20°C/min). Moreover, the measurement was continued even after achievement of the final temperature (180°C) in order to follow the decreasing of the measured specific volume because of the vanishing of the sample's temperature gradient. These experiments were carried out under a pressure of 60 MPa.

Furthermore, specific-volume evolution measurements in isobaric mode were carried out from 220°C to 50°C with four cooling rates (5, 10, 20, and 30°C/min) and under three pressures (40, 80, and 120 MPa).

THERMAL MODELING

For thermal simulations the PVT cell is assumed to be perfect, so two-dimensional thermal effects are considered negligible. In other words, heat transfer is only radial, and the isothermal lines are parallel to the axis of the cylinder. The heat transfer equation that must be solved is expressed as follows:

$$\frac{C_P(P, T)}{V(P, T)} \frac{\partial T}{\partial t} - \frac{\lambda(P, T)}{r} \frac{\partial T}{\partial r} = \frac{\partial}{\partial r}\left(\lambda(P, T) \frac{\partial T}{\partial r}\right) + Q \tag{9}$$

where C_p is the heat capacity, λ is the thermal conductivity, V is the specific volume, and Q is the source term due to the crystallization:

$$Q = \frac{\Delta H_\infty}{V(P, T)} \frac{\partial \alpha}{\partial t} \tag{10}$$

In eq. (10), ΔH_∞ is the total enthalpy of crystallization not considered dependent on the cooling conditions in this work. From the DSC crystallization experiments, the obtained value of ΔH_∞ was 90 J/g.

As already mentioned, variations in relative crystallinity in relation to cooling rate and pressure were taken into account only by a shift on the temperature scale of the primary experimental curve obtained from the DSC measurement (cooling rate: 5°C/min). However, for polypropylene, this simple shift can be considered realistic either for the cooling rate[8–10] or pressure[3,6] effects because the crystallization temperature range itself is narrow and does not broaden much when these parameters are raised. So hereafter, the effects of pressure and cooling rate on relative crystallinity is quantified by a single parameter: the half conversion temperature ($T_{1/2}$) corresponding to the temperature where $\alpha = 0.5$.

Moreover, by analogy with eq. (4), thermal conductivity and heat capacity are obtained from the following mixing rules[11,12]:

$$\lambda(T) = \alpha\lambda_s + (1 - \alpha)\lambda_a \tag{11}$$

with λ_a (W/mK) = $-6{,}25.10{-}5T$ (°C) + 0,189

and λ_s (W/mK) = $-4{,}96.10^{-4}T$ (°C) + 0,31

$$C_p(T) = \alpha C_{ps} + (1 - \alpha)C_{pa} \tag{12}$$

with C_{pa} (J/kgK) = $3{,}10T$ (°C) + 2124

and C_{ps}(J/kgK) = $10{,}68T$ (°C) + 1451

With regard to thermal conductivity, using a simple mixing rule, such as that in eq. (11), may be doubtful since thermal conductivity is not a massive property. But in our case, this aspect can reasonably be considered insignificant. The linear

expressions of eq. (11) were obtained using different measuring methods, as described by Le Bot.[12] The heat-capacity linear relations were obtained from the DSC measurement after subtraction of the crystallization peak. Unfortunately, because of a lack of experimental technique, the effects of the pressure on both heat conductivity and heat capacity have not been quantified. Therefore, the coefficients of eq. (11) and eq. (12) were kept independent of pressure. However, it should remembered that the transition temperature zone's pressure effect has been taken into account by means of the half-conversion temperature variation mentioned before.

The resolution of eq. (9) is achieved using a Crank-Nicholson finite difference scheme. The source term Q is treated by a double iterative scheme, following a method of Huang et al.[13] For reasons of symmetry, the system is only considered along a radius of the cylinder. Its exterior part is submitted to the controlled cooling rate, with a thermal contact resistance equal to 2.10^{-4} Km^2/W. This is a mean value that has been evaluated from injection-molding experiments where thermal contact resistance was identified by an inverse method using heat-flux sensors in the mold.[12] However, it must be pointed out that different values of thermal contact resistance were tested without a significant change in the results.

In eqs. (9) and (10), the specific volume $V(P,T)$ is given by eqs. (4) and (7). Obviously, this specific volume does not equal the measured one because of the thermal gradient in the sample. Indeed, the measured specific volume is an average one, plotted against the temperature at the periphery of the sample. Nevertheless, this average specific volume can be calculated, given that it is the entire volume of the sample divided by the entire mass $\left(L \int_0^R \frac{2\pi r \cdot dr}{V(r)}\right)$, which leads to:

$$\bar{V} = \frac{R^2}{2\displaystyle\int_0^R \frac{r \cdot dr}{V(r)}} \tag{13}$$

The purpose of this study is to compare the experimental data from the PVT100 with the calculated average specific volume, $\bar{V}$. For each pressure and a cooling rate of 10°C/min, $\bar{V}$ was calculated from the starting values of the parameters A_1 to A_4 and $T_{1/2}$ and after the resolution of eq. (9), enabling the temperature profile to be learned each time. Then, the parameters A_1 to A_4 and $T_{1/2}$ were adjusted until agreement between the calculated average specific volume and the experimental one was achieved.

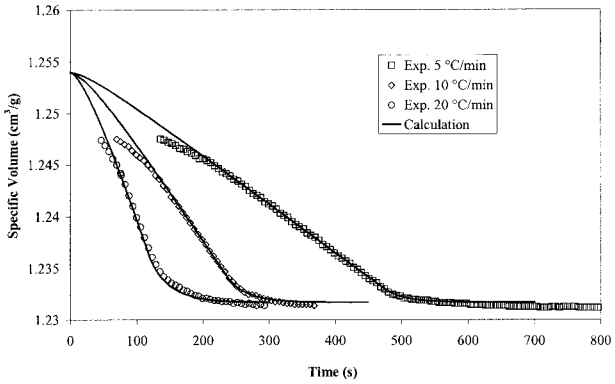

Figure 3 Experimental and calculated evolutions of specific volume versus time for temperature decreasing from 220°C to 180°C at different cooling rates (P = 60 MPa).

RESULTS AND DISCUSSION

As mentioned before, the thermal model was first tested in a temperature range excluding the transition (between 220 and 180°C). In other words, the parameters A_3, A_4, and $T_{1/2}$ vanish in these simulations. However, the experiments, performed under 60 MPa and with different cooling rates, were continued after the achievement of the final control temperature (180°C). The specific volume decrease was recorded until it did not change anymore. Therefore, this final part of the experiment can be used to test the calculation results since stabilization of the measured specific volume when the peripheral temperature is constant directly reflects decreasing of the thermal gradient. The comparison between experimental and calculated results is shown in Figure 3 where specific-volume evolutions versus time are plotted. In this case, the obtained values for the adjusted parameters are:

$$A_1 = 1.131 \text{ cm}^3/\text{g}$$

$$A_2 = 5.575 \times 10^{-4} \text{ cm}^3/\text{g°C} \tag{14}$$

As shown in Figure 3, the model provides a good description of the decrease in specific volume during both cooling and stabilization periods and for

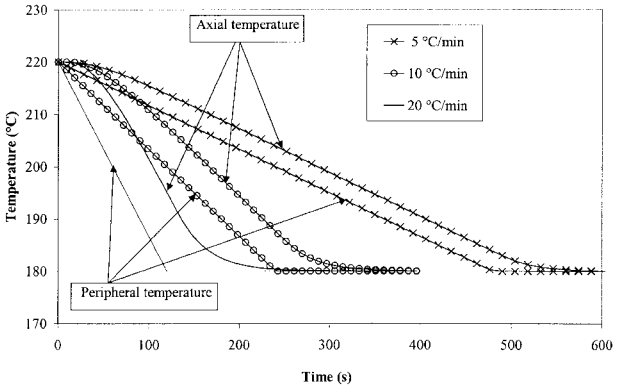

Figure 4 Calculated temperature evolution in the sample for peripheral temperature decreasing from 220°C to 180°C at different cooling rates (P = 60 MPa).

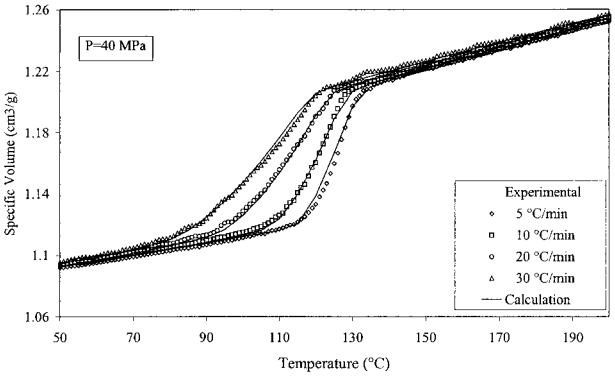

Figure 5 Experimental and calculated average specific volume versus peripheral temperature for different cooling rates (P = 40 MPa)

the three presented cooling rates. Obviously, the employed parameters are the same no matter what the cooling rate.

The evolution of temperature versus time is shown in Figure 4 for the three cooling rates. As can be seen, the difference between the temperature in the sample's axis is greater than the control temperature at the periphery, and the higher the cooling rate, the higher is this difference. Moreover, Figure 4 shows that when the temperature ramp is established in the middle of the sample, the difference between the axial and peripheral temperatures becomes constant, leading to a sliding regime. The establishment of a sliding regime is helpful because it means the cooling rate is the same everywhere in the sample, even if the temperature is not. Therefore, for an analysis of the transition, crystallization temperature can be considered identical for every location in the sample because essentially it depends on cooling rate and pressure. Nevertheless, crystallization time is obviously dependent on location.

The analysis results for measurements including crystallization are displayed in Table I, where the adjusted parameters A_1 to A_4 of eq. (7) and $T_{1/2}$ are reported. Obviously, parameters A_1 to A_4 are only dependent on pressure, but $T_{1/2}$ depends on both pressure and cooling rate.

As an example of the reliability of the results, Figure 5 shows the experimental specific volumes measured under a pressure of 40 MPa for different cooling rates and the average specific volumes calculated with eq. (13). Both these curves are plotted versus the temperature measured at the periphery of the sample. The agreement between measured and calculated curves allows us to conclude that our thermal model is suitable to analyze the experimental results.

Moreover, for the same measurements, the curves described by eq. (4), depending on $T_{1/2}$, and eq. (7), depending on A_1 to A_4, are shown in Figure 6 and compared with the experimental results. As mentioned before, outside the transition zone the calculated specific volume is independent of the cooling rate, leading to a single calcu-

Table I Calculated Coefficients A_1 to A_4 [Eq. 7] and $T_{1/2}$ for Different Pressures and Cooling Rates

P (MPa)		40	60	80	120
A_1 (cm³/g)		1.126	1.131	1.112	1.099
A_2 (cm³/g°C)		6.237×10^{-4}	5.575×10^{-4}	5.107×10^{-4}	4.324×10^{-4}
A_3 (cm³/g)		1.071	/	1.065	1.059
A_4 (cm³/g°C)		4.071×10^{-4}	/	3.066×10^{-4}	2.459×10^{-4}
$T_{1/2}$ (°C)	5°C/min	129.3	/	140.3	150.3
$T_{1/2}$ (°C)	10°C/min	127.3	/	136.8	146.3
$T_{1/2}$ (°C)	20°C/min	123.3	/	/	/
$T_{1/2}$ (°C)	30°C/min	118.8	/	/	/

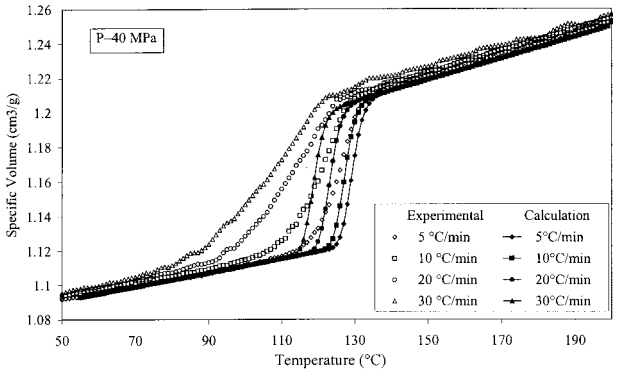

Figure 6 Experimental specific volume versus peripheral temperature for different cooling rates (P = 40 MPa) and calculated specific volume versus temperature without thermal gradient.

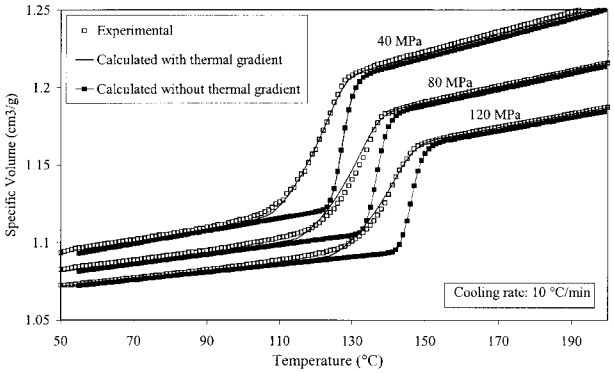

Figure 7 Experimental specific volume versus peripheral temperature for different pressures (cooling rate: 10°C/min) and calculated specific volume versus temperature with or without thermal gradient.

lated curve even if the measured specific volumes exhibit a slight difference because of the thermal gradient. However, in the crystallization zone, the calculated transition is much sharper than the experimental one. Obviously, this difference increases when the cooling rate is higher. One of our first conclusions was that calculating the relative crystallinity curve, $\alpha(T)$, directly from the experimental specific-volume evolution could lead to erroneous results because it would include both crystallization kinetics and thermal gradient effects. Therefore, the calculated coefficients for a crystallization kinetics model such as the Ozawa[14] equation would be irrelevant (for example, the Avrami exponent would probably be too low). In addition, the calculated curves in Figure 6 are different in the crystallization zone because of crystallization temperature dependence on the cooling rate. In other words, the different results for different cooling rates cannot be explained solely by the sample's thermal gradient—a crystallization kinetics effect also must be introduced. In our approach, this effect is taken into account by the half-crystallization temperature variation.

The pressure effect is shown in Figure 7, where calculated and experimental curves for 40, 80, and 120 MPa are plotted for a cooling rate of 10°C/min. Obviously, the crystallization zone is shifted toward the high temperatures when the pressure is increased. From a theoretical point of view, this effect can be easily explained considering the crystallization supercooling ($\Delta T = T_m^0 - T$), which is the difference between the equilibrium melting temperature and the actual crystallization temperature. For a constant cooling rate, crystallization supercooling can be considered identical when the pressure changes because it is the main parameter of the crystallization kinetics.[15] Moreover, because of decreasing liquid-phase entropy, when the pressure increases, the equilibrium melting temperature increases,[16–18] leading to increasing crystallization temperature.

The evolution of $T_{1/2}$ versus the cooling rate is plotted in Figure 8, showing, for example, a decrease of about 10°C when the cooling rate increases from 5°C/min to 30°C/min. This variation is equivalent to the results obtained for a polypropylene by Duffo et al.[9] with DSC at atmospheric pressure.

The variation of $T_{1/2}$ with the pressure (Fig. 9) can be compared with the results of He and Zoller on high-pressure crystallization of polypropylene.[3] Absolute values of the crystallization temperature are of course different from those reported by the authors because crystallization conditions are

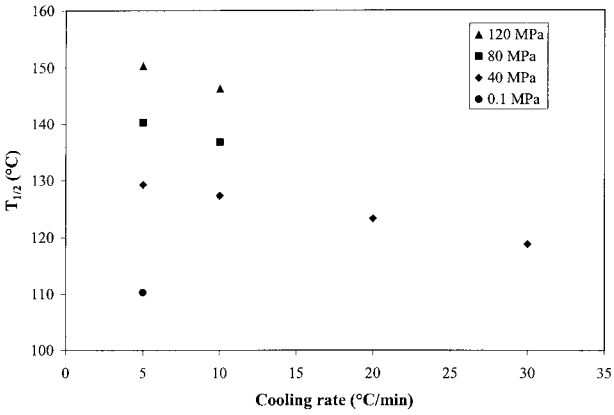

Figure 8 Evolution of half-crystallization temperature versus cooling rate for different pressures.

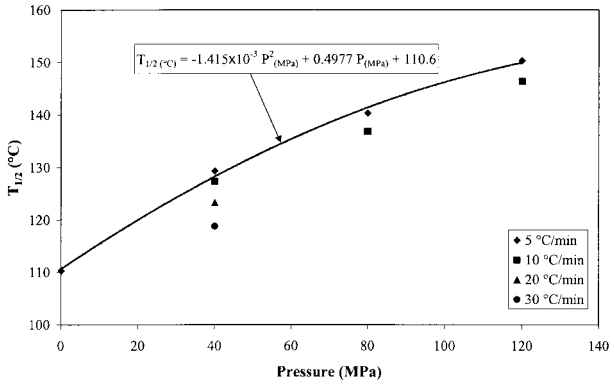

Figure 9 Evolution of half-crystallization temperature versus pressure for different cooling rates. The line shows a second-order polynomial variation fitted on the data for a cooling rate of 5°C/min.

not the same (different PP, different cooling rate). Nevertheless, the variation of crystallization temperature with pressure is comparable, given that it results from the variation of the equilibrium melting temperature (depending only on the nature of the polymer). In our case we obtained a variation of $T_{1/2}$ of about 40°C when the pressure varied from 0.1 to 120 MPa, which is near the variation reported by He and Zoller.

Moreover, the evolution of $T_{1/2}$ with the cooling rate and the pressure can be compared to many results of polypropylene crystallization gathered by Hieber.[19] Even if these results involve different kinds of polypropylene, a general trend has been drawn for the cooling-rate and pressure dependence of $T_{1/2}$, which lead to values very close to the results displayed in Table 1 (within 2°C). For example, at atmospheric pressure this study indicates a $T_{1/2}$ value of 105.5°C for a cooling rate of 30°C/min. In addition, the reported shift due to pressure is 12°C for 400 bars. In Hieber's results the $T_{1/2}$ value calculated at 400 bars and with a cooling rate of 30°C/min is 117.5°C (105.5 + 12), which is close to 118.8°C (see Table I).

CONCLUSIONS

In the case of semicrystalline polymers, crystallization kinetics produces the difficulty in making specific volume measurements. Indeed, the transition temperature depends not only on pressure but also on the entire thermal history (especially the cooling rate). So, it appears the most interesting way to obtain reliable results is to measure the specific volume evolution in cooling and isobaric modes. Thus, thermal-history influence can be analyzed by controlling the cooling rate. Nevertheless, in such conditions, because of poor thermal conductivity of the polymers, an important thermal gradient appears in the sample. So, it is essential to extract the thermal gradient effect from the experimental results in order to obtain the intrinsic specific volume of the polymer and to analyze it in terms of equation-of-state and crystallization kinetics models. In this article thermal analysis of experimental results for a polypropylene shows that when the thermal gradient is taken into account, intrinsic specific volume is very different from direct measurements, especially in the transition zone. Nevertheless, it appears that even on the corrected data, the transition zone is influenced by the cooling rate because of crystallization kinetics. However, our analysis was developed considering a very simple equation of state (linear variation of the specific volume with the temperature outside the transition zone), and an *a priori*-defined relative crystallinity function only shifted in function of the cooling rate and the pressure. Besides, these assumptions are sufficiently realistic for the purpose of this work. Particularly, the calculated transition temperature modification when cooling rate and pressure are changed appears relevant. Nevertheless, the ultimate aim of the study should be the attainment of the relative crystallinity function as an output of the analysis, which is the objective of our future work.

The authors acknowledge Legrand, Moldflow, Plastic Omnium and Solvay for their financial support, and in particular Legrand for its mold manufacturing, Moldflow for the technical support of its software, Plastic Omnium for its mold-deformation FEM calculation, and Solvay for supplying materials and for rheological tests. We also wish to thank H. Alglave, E. Bonneau, P. Kennedy, M. Laplanche, V. Leo, M. Perraudin , J. M. Rossignol, and J. Schoemans for their enriching discussions and help during the entire study.

REFERENCES

1. Zoller, P. J. Polym Sci, Polym Phys Ed 1982, 20, 1453.
2. Wunderlich, B. In Thermal Characterization of Polymeric Materials; E. A. Turi, Ed.; Academic Press: New York, 1981; Chapter 2, p 169.

3. He, J.; Zoller, P. J Polym Sci, Polym Phys Ed 1994, 32, 1049.
4. Lei, M.; Reid, C. G.; Zoller, P. Polymer 1988, 29, 1784.
5. Rodgers, P. A. J Appl Polym Sci 1993, 48, 1061.
6. Hieber, C. A. Intern Polymer Processing 1997, XII(3), 249.
7. Spencer, R. S.; Gilmor, G. D. J Appl Physics 1950, 21, 523.
8. Chan, T. W.; Guo, L.; Isayev, A. I. SPE ANTEC '95 1995, 1476.
9. Duffo, P.; Monasse, B.; Haudin, J. M. J Polym Eng 1991, 10, 151.
10. Kim, Y. C.; Kim, C. Y.; Kim, S. C. Polym Eng and Sci 1991, 31, 1009.
11. Ito, H.; Tsutsumi, Y.; Minagawa, K.; Takimoto, J.-I.; Koyama, K. Colloid Polym Sci 1995, 273, 811.
12. Le Bot, Ph. Ph.D. Thesis, University of Nantes, France, 1998.
13. Huang, H.; Suri, V. K ; Hill, J. L.; Berry, J. T. AFS Transactions 1991, 54.
14. Ozawa, T. Polymer, 12 1971, 150.
15. Hoffman, J. D.; Miller, R. L. Polymer 1997, 38, 3151.
16. Dalal, E. N.; Phillips, P. J. Macromolecules 1984, 17, 248.
17. Phillips, P. J.; Tseng, H. T. Macromolecules 1989, 22, 1649.
18. Kishor, K.; Vasanthakumari, R. High Temperatures—High Pressures 1984, 16, 241.
19. Hieber, C. A. Polymer 1995, 36(7), 1455.